Available online at www.sciencedirect.com
ScienceDirect
Trans. Nonferrous Met. Soc. China 24(2014) 2203−2207
Transactions of Nonferrous Metals Society of China
www.tnmsc.cn

Role of tensile forces in hot tearing formation of cast Al−Si alloy

Rong-fu XU[1], Hong-liang ZHENG[1], Jie LUO[1], Su-pei DING[2], San-ping ZHANG[3], Xue-lei TIAN[1]

1. Key Laboratory for Liquid−Solid Structural Evolution and Processing of Materials (Ministry of Education), Shandong University, Ji'nan 250061, China;
2. Jinan Foundry and Metalforming Machinery Research Institute Co., Ltd., Ji'nan 250022, China;
3. Shandong Shouguang Juneng Special Steel Co., Ltd., Weifang 262711, China

Received 17 October 2013; accepted 16 April 2014

Abstract: The instrumented applied rod casting apparatus (ARCA) was developed to investigate the effects of tensile forces in the hot tearing formation of cast Al−Si alloys. The obtained data of tensile forces/temperature was used to identify hot tearing initiation and propagation and the fracture surface of samples was also investigated. The result shows that the applied tensile forces have a complex effect on load onset for the hot tearing initiation and propagation. During the casting solidification, the tensile forces are gradually increased with the increase of solid fraction. Under the action of tensile forces, there will appear hot tearing and crack propagation on the surface of the sample. When the tensile forces exceed the inherent strength of alloys, there will be fractures on the sample. As for the A356 alloy, the critical fracture stress is about 0.1 MPa. The hot tearing surface morphology shows that the remaining intergranular bridge and liquid films are thick enough to allow the formation of dendrite-tip bumps on the fracture surface.
Key words: hot tearing; tensile force; A356 alloy; aluminum alloy; liquid film; solid fraction

1 Introduction

The cast Al−Si alloys are widely used in the automotive industry due to their excellent casting characteristics and mechanical properties, good corrosion resistance and castability. While the complicated aluminum alloy castings are produced in the factories, some foundry defects, such as shrinkage porosity and hot tearing, are inevitable [1−4]. Once these defects occur especially when the hot tearing occurs, the casting has to be repaired, which leads to immediate productivity loss and raises the cost of production. Therefore, it is necessary to study hot tearing formation in aluminum alloys to prevent this defect in production.

Hot tearing is one of the most serious defects encountered in castings. It is generally considered that it is a spontaneous failure of an alloy during solidification and initiates at the end of solidification in response to localized applied load, strain or strain rate, which may be arisen due to constraint of thermal contraction and the density change from liquid to solid [5−8]. Over years, researchers have devoted to developing various tests to evaluate hot tearing tendency and have made much effort on understanding the fundamentals of hot tearing formation [9]. Various tests and measurement techniques were summarized by ESKIN et al [7] in their reviews, which include the I-beam or backbone mold tests, ring mold tests, cold finger tests and tensile tests etc. In the study of hot tearing of nonferrous binary alloys, many scholars studied Al−Mg, Al−Sn, Al−Cu, Mg−Al and Mg−Zn series alloy and they investigated the effects of alloying elements on hot tearing tendency [10−13]. Above all, these experiments are basically conducted using the alloys which have a high hot tearing tendency or larger solidification range. Nevertheless, for the alloys which have a low hot tearing tendency, the hot tearing defects can also appear in the complicated heavy castings in practical production. Until now, there is no related research in these fields, so it is necessary to study the hot tearing formation of these alloys. And therefore, a widely used aluminum alloy, A356 (Al−7Si−0.3Mg), which is a commercial alloy, was selected in this study.

Foundation item: Project (2011ZX04001-031) supported by National Science and Technology Major Project of "High-end CNC Machine Tools and Basic Manufacturing Equipment", China; Project (51371109) supported by the National Natural Science Foundation of China
Corresponding author: Xue-lei TIAN; Tel: +86-531-88392412; E-mail: tianxuelei@sdu.edu.cn
DOI: 10.1016/S1003-6326(14)63333-1

In the present work, the newly developed applied rod casting apparatus (ARCA) [14] provides the capability to quantitatively monitor hot tearing and evaluate the effects of tensile forces in the hot tearing formation. The microstructure and fracture surface morphology of samples are also investigated.

2 Experimental

2.1 Applied rod casting apparatus

The instrumented applied rod casting apparatus (ARCA) shown in Fig. 1 mainly consists of a mold, a load cell, a load transmission unit, a motor, a data-acquisition system and a steel support plate. The mold is vertically partitioned into two halves. The mold has a modular structure containing changeable inserts to change the dimensions of the mold cavity. The schematic of the mold is shown in Fig. 2. As shown in Fig. 2, the different inner diameters of moveable sleeves can be used. Point *A* (Fig. 2) shows the position of the thermocouple inserted in the mold. To reduce experimental uncertainties, the mold cavity is cleaned and coated with graphite prior to a series of tests. In order to improve heating efficiency, the mold is preheated by resistance copper heaters wrapped with 100 mm-thick insulation board. The casting has one arm, which is constrained by a steel bolt embedded in the end of the casting. The tensile forces are applied in opposite directions by the motor. The hot tearing defect can be induced by this method.

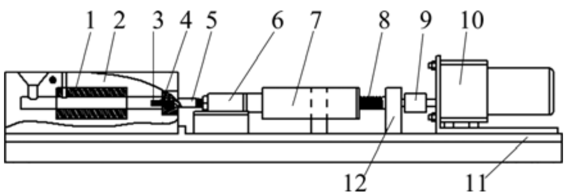

Fig. 1 Schematic of applied rod casting apparatus (front view): 1—Insulating material; 2—Permanent mold; 3—Steel bolt; 4—Graphite stopper; 5—Threaded rod; 6—Load cell; 7—Binding mechanism; 8—Trapezoidal screw; 9—Motor coupling; 10—Adjustable-speed motor; 11—Steel support plate; 12—Bearing block

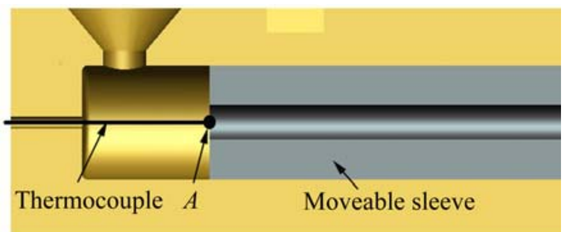

Fig. 2 Schematic of mold used in this study

2.2 Operational procedure

Therefore, a widely used aluminum alloy, A356 (Al−7Si−0.3Mg), which is a commercial alloy, was selected in this study. Its chemical composition determined by optical emission spectroscopy is presented in Table 1.

Table 1 Chemical composition of A356 alloy (mass fraction, %)

Si	Mg	Fe	Ti	Cu	Al
7.18	0.327	0.157	0.0687	0.022	Bal.

The alloy was melted in an electric resistance furnace. For each series of tests, about 1 kg of alloy was prepared. In the study, the pouring temperature was 720 °C and the mold temperature was maintained at 200 °C. The melt was degassed at 700 °C for 10 min with degasifier (C_2Cl_6) to insure minimum hydrogen content. To fully dissolve all the alloying elements, the melt was held at 740 °C for about 20 min before pouring. The melt was stirred for 2 min manually and the oxide layer of the melt was skimmed from the surface. The mold was prepared and preheated to the targeted temperature before pouring. The data acquisition system began to record the temperatures and tensile forces immediately before pouring. When the casting temperature reached the target temperature (20 °C above the eutectic temperature of alloy), unidirectional tensile forces were applied at a predetermined value (the rate of displacement) until the specimen fractured. Each test was repeated 3−5 times.

3 Results and discussion

3.1 Tensile forces and temperature curves

The unidirectional tensile forces were applied at different predetermined rates when the preheated temperature of permanent mold was about 200 °C. Figure 3 shows the typical curves recorded during solidification of A356 alloy with different rates of displacement, where the two samples all fractured. Temperature curves can be used to provide information on the evolution of solid fraction during solidification. The technique is based on the Newtonian method from these cooling curves. The principle of this technique was developed by CHEN and STEFANESCU [15] and described in their work.

When the unidirectional tensile forces were applied at the speed of 0.10 mm/s, the relevant data are shown in Fig. 3(a). From Fig. 3(a), it is observed that the forces started to apply rapidly at 10.2 s and increased with time during entire cooling process. When the forces started to apply, the temperature at the critical region of the sample is 577 °C and the solid fraction is about 0.65. It suggests

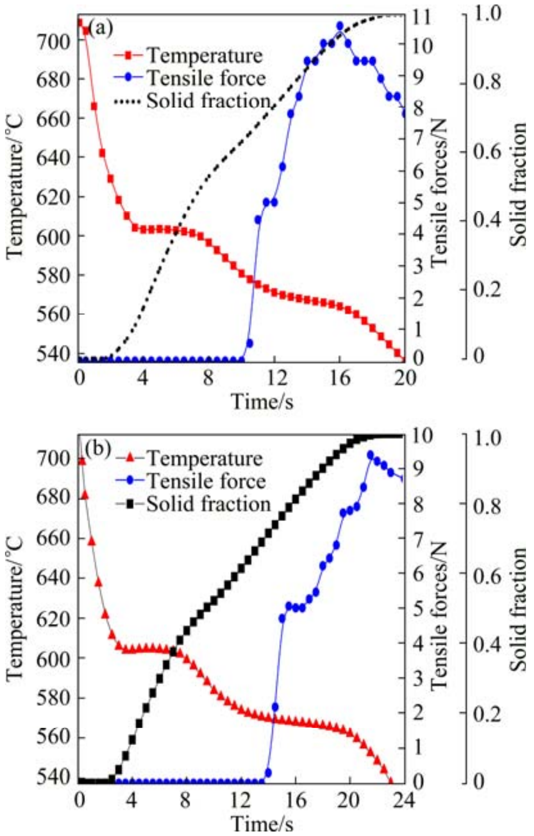

Fig. 3 Tensile force, solid fraction and temperature as function of time for A356 alloy cast at 720 °C with mold temperature of 200 °C and different speeds of displacement: (a) 0.10 mm/s; (b) 0.15 mm/s

that solid skeleton has been formed and the solid network begins to transfer tensile forces at the early stage. An inflection point is observed at 12.1 s in the tensile force curve, which suggests that a continuous dendritic network formed in the mushy zone begins to separate under the applied tensile force. It is indicated that hot tearing is initiating and propagating under the applied tensile force. At this point, the corresponding temperature and solid fraction are 571 °C and 0.73, respectively. It suggests that hot tearing starts to form in the eutectic temperature range. The tensile forces are increased after hot tearing initiation, which suggests that the cracking might partially be filled by remaining liquid in the mushy zone and the tensile strength of solidified part is increased during solidification. The maximum tensile force (10.5 N) is obtained when the solid fraction is around 0.94 and then the tensile force is decreased. At this time the corresponding temperature of the casting is around 564 °C, that is to say, the rod casting completely cracks and the critical fracture stress is about 0.09 MPa when solid fraction is around 0.94. The fracture stress is simply given in the following equation (1):

$$P=F/S \tag{1}$$

where P is the fracture stress; F is the applied tensile force; S is the effective cross-section of fracture area.

When the unidirectional tensile force is applied at the speed of 0.15 mm/s, the hot tearing also appears. The relevant data are shown in Fig. 3(b). Compared with Fig. 3(a), the development of the temperature, tensile force and solid fraction in Fig. 3(b) reveals a similar varying tendency. When the force started to apply, the temperature at the critical region of the sample is 572 °C and the solid fraction is about 0.69. An inflection point is also observed in the tensile force curve. At this point the corresponding temperature and solid fraction are 568 °C and 0.81, respectively. The maximum tensile force (9.59 N) is obtained when the solid fraction is around 0.99 and then the tensile force is decreased. At this time the corresponding temperature of the casting is around 559 °C, that is to say, the rod casting has completely cracked and the critical fracture stress is about 0.10 MPa when the solid fraction is around 0.99.

3.2 Hot tearing surface analysis

Figure 4 shows the typical hot tearing of rod casting. Severe tear is the tear which extends over the entire circumference of the bar. Complete tear is a complete or almost complete separation of the bar. As shown in Fig. 4, it is obvious that the hot tearing occurred at the junctions of the rod casting due to high local stress concentration mainly induced by applied tensile force. The fracture surface is sectioned from the cracking rod casting and then used to analyze the fracture morphology. Figure 5 shows SEM images of the hot tearing fracture surface. The hot tearing fracture surface includes rounded particles of phases and frozen eutectic liquid distributed

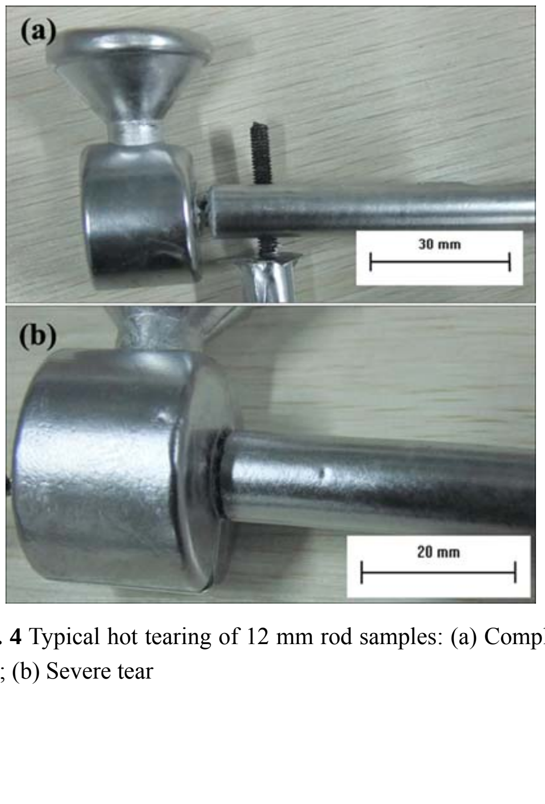

Fig. 4 Typical hot tearing of 12 mm rod samples: (a) Complete tear; (b) Severe tear

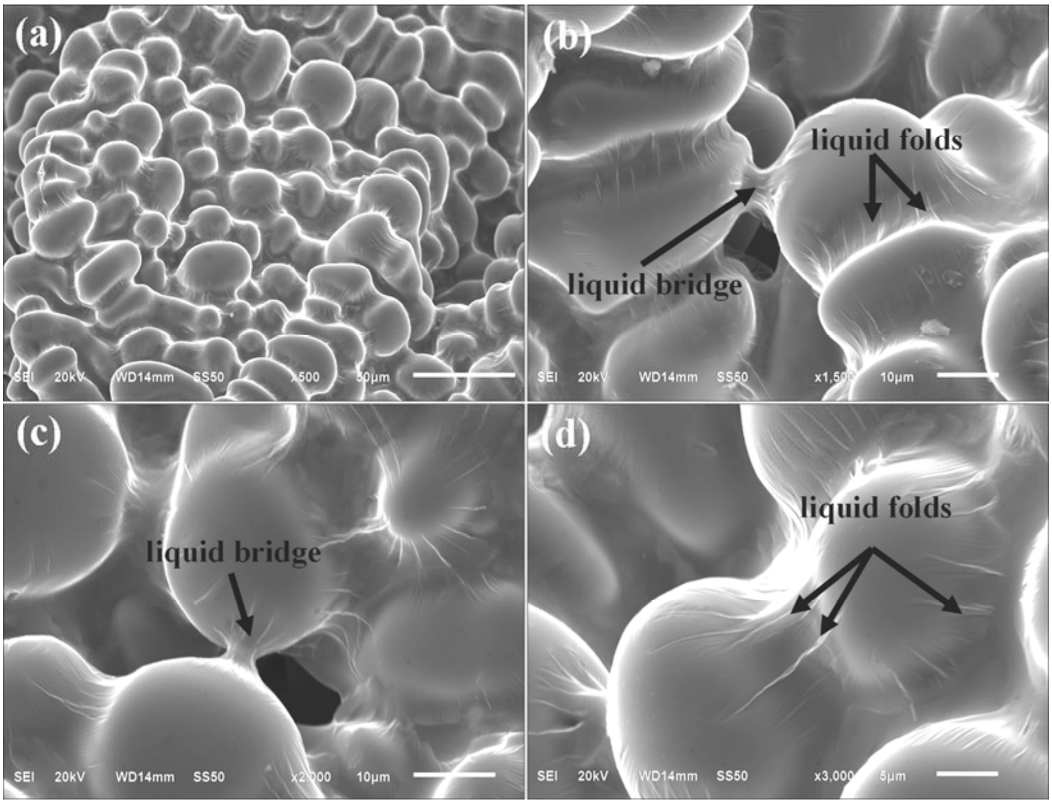

Fig. 5 SEM images of hot tearing fracture surface of 12 mm rod samples for A356 from ARCR: (a) Main fracture morphology of fracture surface; (b, c, d) Feature of liquid bridge and liquid folds on fracture surface

over primary aluminum dendrites. As shown in Fig. 5, a significant amount of liquid film and dendritic bridge are still present on the fracture surface when the hot tearing occurred.

The hot tearing surface morphology shows that the remaining intergranular liquid film is thick enough to allow the formation of dendrite-tip bumps on the fracture surface. The appearances of folds indicate that the surrounding liquid cannot fill the gap among dendrites. At high solid fraction, the solid grains are separated by the remaining liquid films, voids or pores tend to nucleate and then grow into tears under an applied force or shrinkage. During the casting solidification, the solid skeletons begin to grow. Under the action of tensile force, the tensile deformation of the solid skeleton is perpendicular to the growing dendrites and for the induced interdendritic liquid feeding, if the tensile force exceeds the strength of solid skeleton, the intergranular separation will be formed. There is insufficient bulk or interdendritic feeding to compensate for the shrinkage. So, the interdendritic separation is developed to the hot tearing. The remaining intergranular bridge and liquid film separated the feeding channel and they are thick enough to allow the formation of dendrite-tip bumps on the fracture surface. The presence of dendritic bridge or liquid films on the fracture surface is good evidence to support this idea.

4 Conclusions

1) As for the alloys with low hot tearing tendency, the applied tensile force has a complex effect on load onset in the hot tearing initiation and propagation and the tensile force gradually increases with the increase of solid fraction.

2) Under the action of tensile force, the hot tearing initiates and propagates to fracture when the tensile force reaches the maximum value. As for the A356 alloy, the complete hot tearing maybe occurs when the local stress exceeds the strength of solid skeleton, and the maximum fracture stress is about 0.1 MPa.

3) The hot tearing surface morphology shows that the remaining inergranular liquid film and liquid bridge are thick enough to allow the formation of dendrite-tip bumps on the fracture surface.

References

[1] CESCHINI L, MORRI A, MORRI A, GAMBERINI A, MESSIERI S. Correlation between ultimate tensile strength and solidification microstructure for the sand cast A357 aluminium alloy [J]. Materials & Design, 2009, 30: 4525−4531.

[2] THIUGNANAM A, SUKUMARAN K, PILLAI U T S, RAGHUKANDAN K, PAI B C. Effect of Mg on the fracture characteristics of cast Al−7Si−Mg alloys [J]. Materials Science and

Engineering A, 2007, 445−446: 405−414.
[3] JIA Yan-dong, CAO Fu-yang, NING Zhi-liang, SUN Xiao-bing, SUN Jian-fei. Hot deformation behavior of spray formed Al−22Si−5Fe−3Cu−1Mg alloy [J]. Transactions of Nonferrous Metals Society of China, 2011, 21(S): s299−s303.
[4] LI Yuan-yuan, GUO Guo-wen, ZHANG Wei-wen, LUO Zong-qiang. Effects of alloying elements on hot tearing trends of Al−Cu alloy [J]. The Chinese Joural of Nonferrous Metals, 2001, 11(5): 791−795. (in Chinese)
[5] MITCHELL J B, COCKCROFT S L, VIANO D, DAVIDSON C, STJOHN D. Determination of strain during hot tearing by image correlation [J]. Metallurgical and Materials Transactions A, 2007, 38: 2503−2512.
[6] ESTON MARK A, WANG H, GRANDFIELD J, DAVIDSON C J, StJOHN D H, SWEET L D, COUPER M J. Observation and prediction of the hot tear susceptibility of ternary Al−Si−Mg alloys [J]. Metallurgical and Materials Transactions A, 2012, 43: 3227−3238.
[7] ESKIN D G, SUYITNO, KATGERMAN L. Mechanical properties in the semi-solid state and hot tearing of aluminium alloys [J]. Progress in Materials Science, 2004, 49: 629−711.
[8] ESKIN D, DU Q, RUVALCABA D, KATGERMAN L. Experimental study of structure formation in binary Al−Cu alloys at different cooling rates [J]. Materials Science and Engineering A, 2005, 405: 1−10.
[9] ESKIN D G, KATEGERMAN L. A quest for a new hot tearing criterion [J]. Metallurgical and Materials Transactions A, 2007, 38: 1511−1519.
[10] SHI Zhao-xia, DONG Jian-xin, ZHANG Mai-cang, ZHENG Lei. Hot tearing susceptibility analysis and prediction of K418 superalloy for auto turbocharger turbine wheel [J]. The Chinese Journal of Nonferrous Metals, 2013, 23(1): 82−90. (in Chinese)
[11] LEMIEUX A, LANGLAIS J, BOUCHARD D, GRANT CHEN X. Effect of Si, Cu and Fe on mechanical properties of cast semi-solid 206 alloys [J]. Transactions of Nonferrous Metals Society of China, 2010, 20: 1555−1560.
[12] NABAWY A M, SAMUEL A M, SAMUEL F H, DOTY H W. Influence of additions of Zr, Ti−B, Sr, and Si as well as of mold temperature on the hot-tearing susceptibility of an experimental Al−2%Cu−1%Si alloy [J]. Journal of Materials Science, 2012, 47: 4146−4158.
[13] GUNDE P, SCHIFFL A, UGGOWITZER P J. Influence of yttrium additions on the hot tearing susceptibility of magnesium–zinc alloys [J]. Materials Science and Engineering A, 2010, 527: 7074−7079.
[14] XU Rong-fu, ZHENG Hong-liang, GUO Feng-xiang, DING Su-pei, TIAN Xue-lei. A new investigated method on hot tearing behavior in aluminum alloys [J]. Russian Journal of Non-Ferrous Metals, 2013, 54: 377−382.
[15] CHEN I G, STEFANESCU D M. Computer-aided differential thermal analysis of spheroidal and compacted graphite cast irons [J]. Transactions of the American Foundrymen's Society, 1984, 92: 947−964.

拉力在铸造铝硅合金热裂形成过程中的作用

许荣福[1]，郑洪亮[1]，罗 杰[1]，丁苏沛[2]，张三平[3]，田学雷[1]

1. 山东大学 材料液固结构演变与加工教育部重点实验室，济南 250061；
2. 济南铸造锻压机械研究所有限公司，济南 250022；
3. 山东寿光巨能特钢有限公司，潍坊 262711

摘　要：利用 A356 合金研究拉力在热裂的形成及其断裂行为中的作用。利用一个新型的实验装置进行相关实验研究。该实验装置能够同时测量并采集受限试样在凝固过程中施加的拉力和温度的数据。这些数据可以用来研究热裂的萌生和扩展。研究了在不同加载速度下，固相率的演变和热裂的形成之间的定量关系。由实验结果可知，施加的拉力在热裂萌生初期起着复杂的作用。在合金凝固过程中，随着固相率的不断增加，拉力会逐渐增大直至最大值，然后急剧下降，此时试样出现裂纹并在拉力的持续作用下产生断裂。对于 A356 合金，产生早高温下产生断裂的临界应力是 0.1 MPa。由热裂纹的断口形貌可知，在凝固末期形成的晶间搭桥和液膜褶皱对热裂的形成起重要的作用。

关键词：热裂；拉力；A356 合金；铝合金；液膜；固相率

(Edited by Hua YANG)